ANALYSIS AND PREDICTION OF SIZE EFFECT ON LASER FORMING OF SHEET METAL

Peng Cheng, Y.Lawrence Yao, Chao Liu, Duncan Pratt, Yajun Fan
Department of Mechanical Engineering
Columbia University, New York, NY 10027

KEYWORDS

Size Effect, Laser Forming, Sheet Metal

ABSTRACT

Geometric effects play an important role in laser forming process; however, few investigations have been reported on the geometric size effect other than sheet thickness. In this paper, the influence of size effect, including sheet width and sheet length, on laser induced deformation is experimentally, numerically and analytically investigated. A size matrix is designed to cover a wide range of sheet width and length for experiments and numerical simulation. Distinctive trends in bending angle are observed for varying sheet width, length or both. The results are interpreted in terms of heat sink effect and bending non-uniformity. An analytic model is developed to facilitate size effect prediction. The model is based on the solution to a moving strip heat source over a finite size sheet and on the account for pre-bending effect among consecutive segments on the scanning path. It is compared with an existing analytical model and numerical simulation.

INTRODUCTION

Laser forming is a flexible forming process that forms sheet metal by means of stresses induced by external heat instead of external force. Understanding various aspects of laser forming has been a challenging problem of considerable theoretical and practical interest. The relationships of bending distortion and process parameters, material properties and workpiece thickness have been developed in analytical models. Additional information, such as influence of strain hardening, strain rate effects and edge effect have also been reported in experimental and numerical investigations.

The geometric effects in laser forming, however, have not been fully studied. Most studies focused on the effect of workpiece thickness without considering other geometric attributes. Scully (1987) proposed that plate thickness s_0 is one of the primary factors in laser forming and he adopted a quantity $P/(s_0\sqrt{V})$ that was used in arc welding to study the effect of plate thickness on bending angle, but he did not give an exact relationship between them. Koloman and Karol (1991) proposed an analytical model in which the bending angle is a function of the reciprocal of the square of thickness. However, the bending angles calculated from this formula are some orders of magnitude too large compared with experiments. Vollertsen (1994a, 1994b) proposed a simple two-layer model based on the

temperature gradient mechanism (TGM) assumption. Due to the assumption that bending deformation is uniform along the sheet length, the only geometric factor appeared in those models is plate thickness.

Experimental investigations and numerical simulation, however, have shown that sheet size has an effect on laser forming. Vollertsen (1994a) pointed out that the width of the sheet influences the cooling conditions and therefore the bending angle, and he also observed the influence of the sheet length on stress state. But he did not consider the size influences in his analytical solutions. Hsiao, et al. (1997) have found that for Inconel 625 the angular distortion increases as sheet length increases and he proposed the reason is the longer plate provides more cold metal to produce thermal stresses. He also proposed that there is an upper limit in the angular distortion with respect to the sheet length. However, these investigations on size effect are empirical and did not lead to analytical prediction.

In this paper, the size effect exhibited in laser forming process is investigated. First the experimental and numerical investigations aimed at advancing the understanding of the causes of the size effect in the straight-line laser forming are presented for a wide range of sheet sizes. Various deformation patterns due to the size effect are explained. To better quantify the role of size effect on laser forming, a predictive model is developed, in which finite sheet width and length are considered. The proposed model is experimentally validated.

EXPERIMENTS AND SIMULATION

Experiments of straight-line laser forming (Figure 1) were carried out with the sheet length and width varying from 80 mm to 200 mm, in which the size effect was investigated in three cases: varying sheet width, varying sheet length, and varying square size. Additional set of samples (*L* = 20~60 *mm*, *W* = 80 *mm*) were also used to further investigate the sheet length effect because it was reported (Vollertsen, 1994a) that the effect of sheet length is more pronounced when length-to-thickness ratio (L/s_0) is small. The sheet thickness is fixed at 0.89 mm since effect of thickness has been well studied as discussed in the previous section. The sheet material is AISI 1010 steel. The laser system used in the experiments is a PRC-1500 CO_2 laser, with a maximum output power of 1.5 Kw and power density distribution was TEM_{00}. The diameter of the laser beam used is 4mm.

In numerical simulation the laser forming process is modeled as a sequentially coupled thermal-mechanical process. More details about the thermal model can be found in Cheng and Yao (2003). In the mechanical analysis, direct integration is used for the nonlinear transient dynamic response. The body force at a point can be expressed in the virtual work equation as

$$\int_V \mathbf{f}\cdot\delta\mathbf{v}dV = \int_V \mathbf{F}\cdot\delta\mathbf{v}dV - \int_V \rho\ddot{\mathbf{u}}\cdot\delta\mathbf{v}dV \qquad (1)$$

where **f** is the body force, $\delta\mathbf{v}$ the "virtual" velocity field, V the volume, **F** the externally prescribed force, ρ the density of the material, $\ddot{\mathbf{u}}$ the acceleration field. With the nodal interpolation, the inertia force is $-(\int_{V_0}\rho_0\mathbf{N}^N\cdot\mathbf{N}^M dV_0)\ddot{u}^M$; that is, the consistent mass matrix times the accelerations of the nodal variables ($\ddot{u}^M$), where $\mathbf{N}^N$ or $\mathbf{N}^M$ (*N, M*=1,2,…up to the total number of variables in the problem) is a set of N vector interpolation functions, ρ_0 and V_0 the reference density and reference volume, respectively..

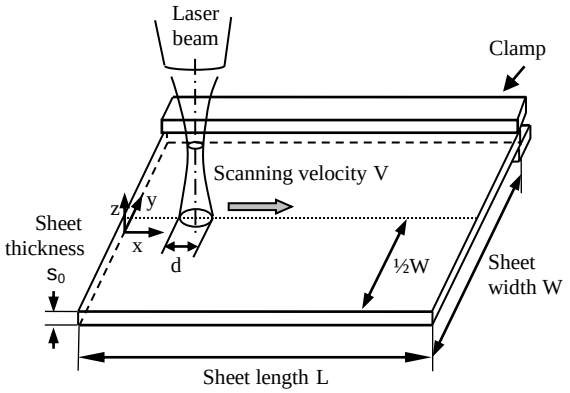

FIGURE 1 SHEMATIC OF STRAIGHT-LINE LASER BENDING

ABAQUS was used to complement the numerical simulation. A quadratic 20-node brick element was used in the mechanical analysis because this kind of element has no shear locking and hourglass stiffness and is also suitable for bending-deformation-dominated processes such as laser forming. A user subroutine of dflux was developed to model the heat source input from the Gaussian laser beam.

EXPERIMENTAL AND NUMERICAL RESULTS AND DISCUSSIONS

.

Effect of Sheet Width

Figure 2 shows the variation of bending angle with the sheet width varying while the sheet length being constant. Good agreement has been obtained between the simulation and the experiment. It is seen from that, for low carbon steel, when the sheet width increases, bending angle decreases. This differs from the observation on LF of Inconel 625 (Hsiao, et al., 1997), where it was reported that bending angle increases with both sheet width and sheet length and it was attributed to larger thermal stress caused by larger constraint from the cold plate. The discrepancy is indicative that the size effect on bending angle may not be as simple as it was proposed.

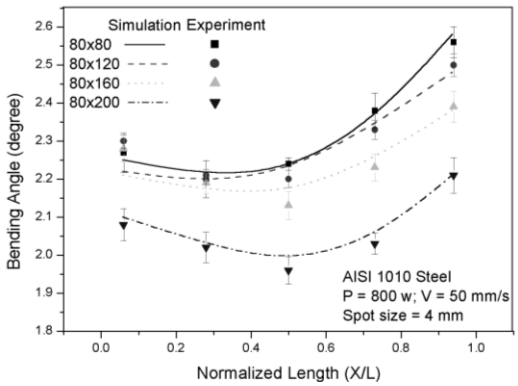

FIGURE 2 EXPERIMENTAL AND NUMERICAL RESULTS FOR DIFFERENT SHEET WIDTH

When the sheet width varies, both thermal conduction condition and sheet weight vary. In numerical simulation, the weight effect was removed by deleting the gravity term in the model. Figure 3 shows the bending angle difference between models with or without considering the gravity. It is found that, for the sheet width range investigated, the bending angle difference caused by gravity is almost the same for 80x80 and 80x200 samples, which clearly indicates that the gravity effect is not the major reason for the bending angles change caused by sheet width change. Further evidence was obtained by examining the *Z*-direction stress at a typical point and it is found that gravity does not affect the bending stress significantly even the sheet width increases from 80 to 200mm. So the reason of bending angle difference caused by different width may lie in the thermal conduction condition.

Figure 4 shows the simulated time history of temperature. It is seen that the peak temperature at the top surface of workpiece drops when the sheet width increases, while the temperature at the bottom surface is almost the same. The reduced temperature gradient in the thickness direction is clearly responsible for the reduced bending angle when sheet width increases. This is obviously due to the fact that a larger width provides a larger heat sink.

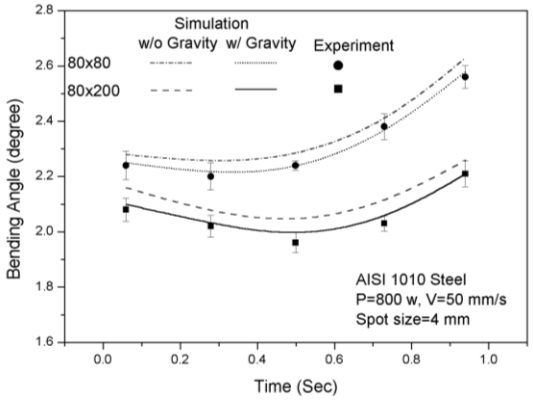

FIGURE 3 INFLUCENCE OF GRAVITY ON BENDING ANGLE WHEN THE SHEET WIDTH VARIES

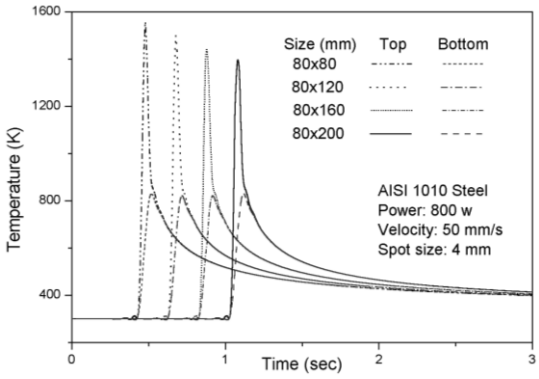

FIGURE 4 SIMULATED TIME HISTORY OF TEMPERATURE FOR DIFFERENT SHEET WIDTH (0.2 SECONDS TIME DELAY BETWEEN EACH CASE FOR VIEWING CLARITY)

Effect of Sheet Length

Figure 5 shows that the bending angle increases with sheet length. Figure 6 shows temperature on the top and bottom surfaces of workpiece. It is seen that although the sheet

length increases, the thermal field is not visibly affected. This is primarily because the heat sink effect discussed above is over shadowed in the direction of sheet length by the fast moving laser beam along the same direction.

Figure 7 shows the time history of bending angle, peak temperature, and *Z*-direction stress in a 200x80 size sample at a typical position (x = 61.3 mm). It is seen that before the laser beam reaches that point (signified by the rapid rise of temperature), the bending angle has reached about 1/3 of the final bending angle. When the

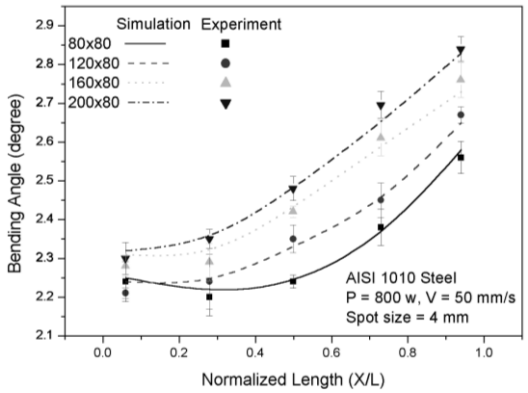

FIGURE 5 EXPERIMENTAL AND NUMERICAL RESULTS FOR DIFFERENT SHEET LENGTH

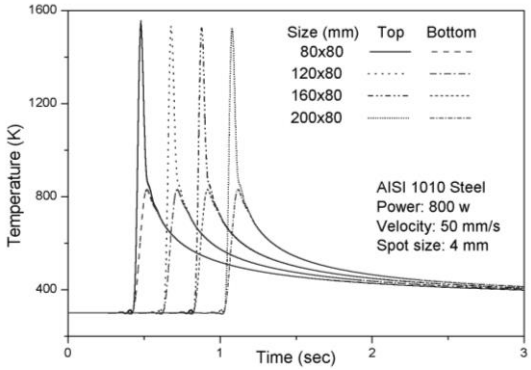

FIGURE 6 SIMULATED TIME HISOTRY OF TEMPERATURE FOR DIFFERENT SHEET LENGTH (0.2 SECOND TIME DELAY BETWEEN EACH CASE FOR VIEWING CLARITY)

laser beam reaches that point, the bending angle increases rapidly approximately until the *Z*-direction stress stabilizes. The bending angle continues to rise slowly after the laser passes to the point. The existence of the pre-bending (bending at a location generated before the heat source arrives at the location) and post-bending (bending at a location generated after the heat source passes the location) obviously plays an important role in creating the final bending angle. It is also found that there is more pre-bending effect in the shorter sheet (80x80) than in the longer sheet (200x80), and the opposite can be said about the post-bending effect. In any case, within the sheet length range investigated, the pre-bending effect is more significant than the post-bending effect.

Varying Square Sizes

Figure 8 shows the average bending angle trends in case of varying width, length and both. It is seen that for the varying square sizes, the bending angle increases before it decreases. This is clearly because of the competing effects of heat sink primarily associated with sheet width and the pre-/post-bending effect primarily associated with sheet length. The pre-/post-bending effect is more dominant initially and as a result the bending angle increases before heat sink effect takes over and thus the bending angle decreases**.**

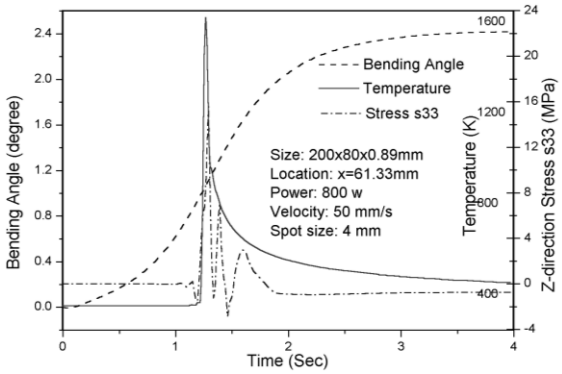

FIGURE 7 SIMULATED TIME HISTORY OF BENDING ANGLE, TEMPERATURE AND STRESS

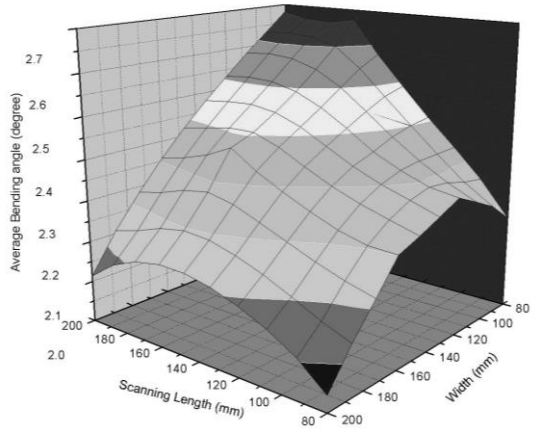

FIGURE 8 AVERAGE BENDING ANGLE INFLUENCED BY SHEET SIZE EFFECT

Inertia effect

To investigate size effect on bending angle, inertia effect needs to be examined since it varies with sheet size. It was found that the static model, in which the inertia effect is ignored, underestimates the bending angle. This is because the inertia force considered in the dynamic model makes the bending force larger and thus the bending angle larger than that of static model. It was also found that when sheet width increase, the bending angle difference between the dynamic and static model decreases. This is because the inertia force is mainly dependent on the difference between laser-induced thermal load and gravity effect. When the sheet width increases, the inertia force decreases due to the larger gravity and the smaller thermal load caused by larger heat sink effect. When sheet length increases, the inertia effect increases due to the more dominant thermal load due to the longer heat input path.

PREDICTIVE MODEL DEVELOPMENT

As mentioned before, laser forming is a fully coupled, non-linear, thermo-mechanical process, and is often simulated by a full three-dimensional finite element method. However, analytical models are more intuitive and depict the cause-effect relations directly. But considerable simplifications are required to succeed in developing such analytic models. The objective of this section is to develop an analytic model which can predict the size effect on bending angle by properly balancing between essential simplifications and model fidelity.

Existing Analytical Models and Proposed Approach

The most widely used model is perhaps the one developed by Vollertsen (1994), which assumes the temperature gradient mechanism (TGM)

$$\alpha_B = \frac{3 l_h \alpha_{th} \Delta T}{2 s_0} \tag{2}$$

where α_B is bending angle, l_h is the width of a heated zone, α_{th} is the thermal expansion coefficient, ΔT is the temperature rise in the heated zone, and s_0 is the sheet thickness. This model was arrived at by using a two-layer assumption. The bending angle is assumed to occur at once and therefore is uniform along the scanning path.

The thermal field is obtained by

$$\Delta T = \frac{2AP}{V c_p l_h s_0 \rho} \tag{3}$$

where A is absorption coefficient, *P* is laser power, *V* is laser scanning velocity, c_p is heat capacity, and ρ is the density. Heat conduction is not considered in Equation 2.

To take into account of heat conduction, Scully (1987) and Masubuchi (1992) adopted the solution to the moving line heat source problem (Rosenthal, 1947) to determine ΔT

$$\Delta T(r) = \frac{q}{\pi k g} e^{-\lambda V \xi} K_0(\lambda V r) \tag{4}$$

where q is power of the line source, *g* is the height of the line source, k is thermal conductivity, $\lambda = 1/(2\kappa)$ and κ is diffusivity, *V* is the moving speed along the *x*-axis, $\xi = x - Vt$ is the distance to the heat source along the moving path, r is the distance to the source center in scanning plane, K_0 is modified Bessel function of type zero. Eq. 4, however, is obtained based on infinite boundary condition and is not suitable for investigating the size effect.

As experimentally and numerically shown early, the sheet width effect on bending angle is primarily associated with the heat sink effect, while the sheet length effect is primarily associated with pre-/post-bending effect. The proposed approach in this paper consists of (1) derivation of an ΔT expression for finite sheet width *W*, taking into account of the finite laser beam size; and (2) adaptation of Eq. 2 for a small length of the scanning path (instead of the entire scanning path) and derivation of an α_B expression for the scanning length *L*.

Thermal Effect

The finite width condition is introduced in the solution of the moving line heat source (Eq. 4) by the method of images (Rosenthal, 1947),

$$\Delta T = \frac{q}{\pi k g} e^{-\lambda V \xi} \sum_{n=-\infty}^{n=+\infty} K_0(\lambda V r_n) \tag{5}$$

Taking into account of the finite boundary condition $\partial T / \partial y \to 0$ as $y = 0$ and $y = a = W/2$, a solution can be obtained by transforming Equa-

tion (5) into a Fourier series. The obtained solution, however, is based on a line source without any line width and the temperature value at the source center is infinite. To avoid this, an assumption that the line source has a finite width is made and this assumption is realistic for the laser beam source. It is assumed the moving line source has a width which equals to the laser beam diameter on the sheet. By a series of derivation, the temperature within the line width $-d/2 < \xi < d/2$ is

$$\Delta T = \frac{q}{\rho c_p agVd}[\frac{1}{2\lambda V} + (\frac{d}{2} - \xi) - \frac{e^{-2\lambda V(d/2+\xi)}}{2\lambda V} + \sum \frac{2}{\mu_n(\mu_n+1)} \cdot \frac{1-e^{-(\mu_n+1)\lambda V(d/2+\xi)}}{\lambda V} \cos\frac{n\pi y}{a} + \sum \frac{2}{\mu_n(\mu_n-1)} \cdot \frac{1-e^{(\mu_n-1)\lambda V(\xi-d/2)}}{\lambda V} \cos\frac{n\pi y}{a}] \quad (6)$$

where *g* is the height of the line source (equal to half of the sheet thickness under the two-layer assumption), and $\mu_n = \sqrt{1+(\frac{\pi n}{\lambda V a})^2}$. Please note that ΔT is now a function of sheet width *a*. To obtain a representative ΔT for the two-layer model (Eq. 2), the temperature increase in the square domain of l_h is averaged.

From the calculated temperature at the heat source center by the analytic model, the decreasing trend with increasing sheet width is observed and is consistent with FEM simulation results. There is some discrepancy in slope likely due to the several assumptions underlying the proposed analytic model, such as temperature independent material properties and the two-layer assumption.

Mechanical Effect

As shown before, the sheet length effect on bending angle can be accounted for primarily through the pre-/post-bending effect along the scanning path, and the pre-bending is more dominant than the post-bending in creating the final non-uniform bending angle. Therefore, only pre-bending is considered in the following derivation.

To consider the non-uniform bending along the scanning path, the scanning length *L* is divided into *n* segments. Each segment is *L/n* long and assumed to have a uniform bending along the segment (Fig. 9). For the segments that heat source has passed, permanent plastic deformation occurs. For those segments that heat source has not arrived, no plastic strain occurs and only the segment following the plastic-deformed segments is affected by the previous segment.

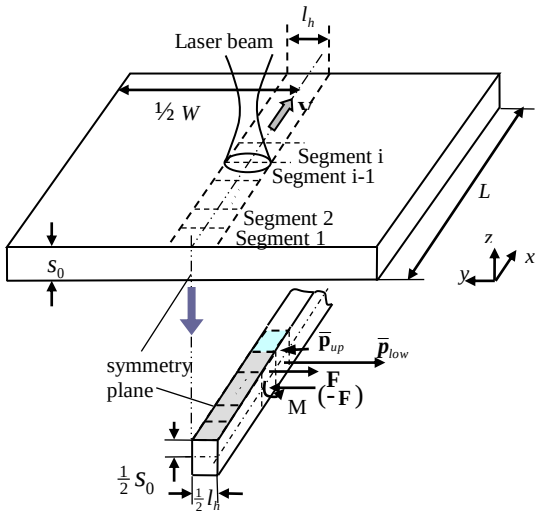

FIGURE 9 SCHEMATIC OF MECHANICAL MODEL

Starting the analysis from the first segment, since no pre-bending effect, the bending angle in the first segment can be obtained through a two-layer assumption (Vollertsen, 1994a), that is

$$\alpha_1 = \frac{2l_h(\varepsilon_{low} - \varepsilon_{up})}{s_0} \quad (7)$$

where ε_{up} and ε_{low} are strains of the upper and lower layer, respectively. Assuming that the thermal expansion is fully converted into the plastic compression, we have

$$\varepsilon_{up} = \varepsilon_{el} + \varepsilon_{pl} = (\frac{F}{EA} - \frac{M}{EI}\frac{s_0}{2}) + (-\alpha_{th}\Delta T) \quad (8)$$

$$\varepsilon_{low} = -\varepsilon_{el} = -\frac{F}{EA} + \frac{M}{EI}\frac{s_0}{2} \quad (9)$$

where F and M are the force and moment caused by difference in compression between the upper and lower layer of the segment, E is the elastic modulus, A is the cross-sectional area of each layer of the segment and $A = \frac{1}{2}s_0\frac{L}{n}$, and I is the inertia momentum and $I = \frac{1}{12}\frac{L}{n}s_0^3$. Substituting Eqs 8 and 9 into Eq. 7 and noting the equilibrium equation $F \cdot \frac{s_0}{2} = M = \frac{EI}{l_h}\alpha_1$, it is obtained that

$$\alpha_1 = \frac{3 l_h \alpha_{th} \Delta T}{2 s_0} \equiv \alpha \quad (10)$$

and $$\varepsilon_{el} = -\frac{1}{4}\alpha_{th}\Delta T \quad (11)$$

For the second segment that heat source has not reached, elastic strain also occurs due to the compatibility. The elastic strain at the boundary between the first segment and the second segment equals to the elastic strain of the first segment, and the elastic stain at the boundary between the second segment and the third segment is zero. So the average elastic strain in the second segment (the affected segment) is

$$\bar{\varepsilon}_{up} = \frac{1}{2}\varepsilon_{el} = -\frac{1}{8}\alpha_{th}\Delta T$$

$$\bar{\varepsilon}_{low} = -\frac{1}{2}\varepsilon_{el} = \frac{1}{8}\alpha_{th}\Delta T \quad (12)$$

Then the equivalent elastic forces on the upper and the lower layer of the second segment are

$$\bar{p}_{up} = EA\bar{\varepsilon}_{up} = -\bar{p}_{low} \quad (13)$$

And it can be assumed that the forces are loaded at the center point of each applied plane.
Then the pre-bending angle of the second segment can be obtained:

$$\Delta\alpha_1 = \frac{p_{up} \cdot \frac{1}{2} s_0}{EI} l_h = \frac{3}{8}\frac{l_h}{s_0}\alpha_{th}\Delta T = \frac{1}{4}\alpha_1 \quad (14)$$

The final bending angle of the second segment equals to the summation of the bending angle caused by heat flux and the pre-bending angle:

$$\alpha_2 = \alpha + \frac{1}{4}\alpha_1 \quad (15)$$

In the similar way, when the heat source moves out of the second segment and has not entered the third segment, the pre-bending angle of the third segment is $\frac{1}{4}\alpha_2$, where α_2 is the bending angle of the second segment. Similarly, the bending angle of the i-*th* segment is

$$\alpha_i = \alpha + \frac{1}{4}\alpha_{i-1} \quad (16)$$

where α_{i-1} is the bending angle of the (*i*-1)th segment. Then the average bending angle of a plate with the length of *L* and consisting of *n* segments is

$$\bar{\alpha} = \frac{4}{3}[1 - \frac{1}{3n}(1 - \frac{1}{4^n})]\alpha \approx \frac{4}{3}(1 - \frac{1}{3n})\alpha \quad (17)$$

Substituting the expression of α, it is obtained that

$$\bar{\alpha} = (1 - \frac{1}{3n})\frac{2 l_h}{s_0}\alpha_{th}\Delta T \quad (18)$$

where the temperature increment ΔT can be obtained by the thermal model introduced in former section.

Eq. 18 predicts the bending angle of a finite sized sheet. The effect of sheet width is reflected in ΔT and the effect of sheet length is reflected in *n*. To apply Eq. 18 to a specific laser forming process involving a specific material, *n* and l_h need to be determined, both are related to the extent of the plastically deformed zone. Using temperature distributions predicted by the proposed thermal model under various conditions, the range of the plastic-deformed zone in which the temperature is higher than critical temperature (~700K) is approximately determined and related to the line energy *P/V* as

$$l_h \approx 0.125(P/V) + 0.5 \quad (19)$$

$$L/n \approx 3(P/V) - 17.5 \quad (20)$$

In above equations, the unit of length, power and velocity is mm, watt and mm/s, respectively. Substituting Eqs. 19 and 20 into Equation (18), one can predict the bending angle of a finite sized sheet.

Validation of the Predictive Model

Figs. 10 and 11 show the validation of the proposed model. It is seen that the bending angle values obtained from the proposed model show a similar trend as the experiments and simulation, while the existing analytic model is unable to predict the size effect. Although the proposed model over estimates the bending angle, its agreement with experimental and simulation values is significantly better compared with the other analytical model. The main reason for this over estimate comes from the omission of yield strength consideration in the proposed analytical model. The fraction of the heat energy absorbed by the zones, where the heated temperature is below the critical temperature to effect appreciable plastic deformation, is almost 25% of the total input energy (Vollertsen, 1994a), while the model assumes all the input energy is used for deformation.

In the case of varying sheet length, the model predicted trend of bending angle is well agreeable with the experimental and simulation values. The trend is consistent with Vollertsen's (1994a) experimental observations, that is, when the ratio of length and thickness is small, the increasing trend of bending angle with sheet length is

more pronounced and there is an upper limit of bending angle when the sheet length keeps increasing. In the comparison of varying square size, the predictive model also captures the variation trend.

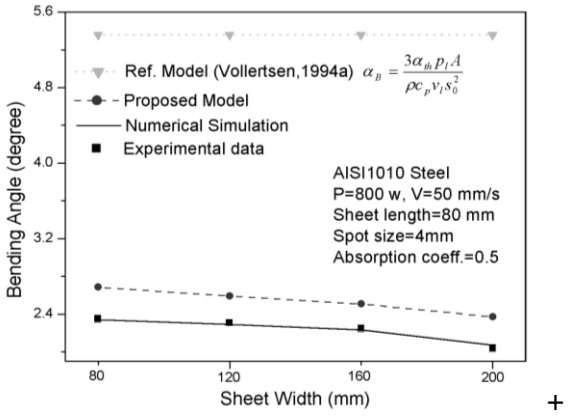

FIGURE 10 ANALYTIC PREDICTION OF BENDING ANGLE FOR VARING SHEET WIDTH

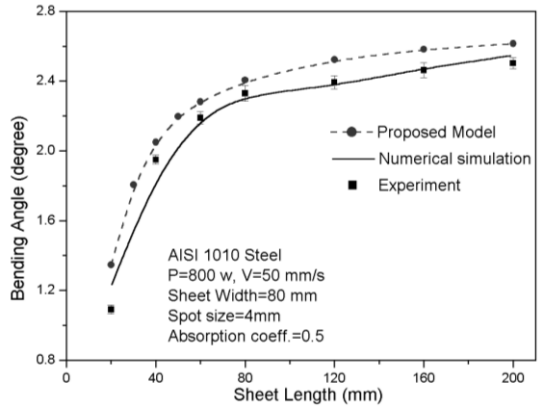

FIGURE 11 ANALYTIC PREDICTION OF BENDING ANGLE FOR VARING SHEET LENGTH

CONCLUSIONS

Within the sheet size range as well as process condition used in this investigation, the size effect on laser forming of low carbon steel sheet can be summarized as follows. When sheet length is constant and sheet width increases, the bending angle slightly decreases. This is primarily due to the increased heat sink effect with sheet width. When sheet width is constant and sheet length increases, the bending angle slightly increases. This is primarily due to the fact that the bending angle along the scanning path is non-uniform and influenced by the pre-/post-bending effect. When both the sheet length and sheet width increase as square sheets, the bending angle increases before decreases due to the competing effects. Based on the experimental and numerical results and physical interpretations above, an analytical model is developed to predict the size effect. Sheet width effect is accounted for by modeling a moving "strip" heat source over a finite width sheet. Sheet length effect is modeled by dividing a finite scanning path into small segments and taking into account the pre-bending effect between consecutive segments. The analytic model compares favorably with the existing analytical model in terms of agreement with experimental measurement and numerical simulation.

REFERENCES

Cheng, P, and Yao, Y. L, (2003), "The Influence of Sheet Metal Anisotropy on Laser Forming Process," *Proceedings of ICALEO'03*, Section E, pp.1-10.

Koloman, K., and Kraol, P., (1991), "Formen durch locale Erwarmung," *Metal Forming-Theory and Practice: Proceedings of the 5th International Conference on Metal Forming,* Tisza, M., and Kardos, K. (Eds), pp. 69-75.

Hsiao, Y. C., Maher, W., et al., (1997), "Finite Element Modeling of Laser Forming," *Proc. ICALEO'97,* Section A, pp. 31-40.

Masubuchi, K., (1992), "Studies at MIT related to applications of laser technologies to metal fabrication," *Proc. of LAMP'92*, pp. 939-946.

Rosenthal, D., (1947), "The Theory of Moving Sources of Heat and Its Applications to Metal Treatments," *Transactions of the ASME, Journal of heat transfer*, Vol. 68, pp. 849-866.

Scully, K., (1987), "Laser Line Heating," Journal of Ship Production, Vol. 3, No. 4, pp. 237-246.

Vollertsen, F., (1994a), "An Analytical Model for Laser Bending," *Lasers in Engineering,* Vol. 2, pp. 261-276.

Vollertsen, F., (1994b), "Mechanisms and Models for Laser Forming," *Laser Assisted Net Shape Engineering, Proc. of the LANE'94*, Vol. 1, Meisenbach Bamberg, pp. 345-360